Optica Applicata, Vol. XXX, No. 2–3, 2000

Compression of greyscale images based on sub-band decomposition using morphological filters

JACEK PNIEWSKI, TOMASZ SZOPLIK

Institute of Geophysics, Warsaw University, ul. Pasteura 7, 02–093 Warszawa, Poland.

We present an algorithm for compression of greyscale images, which is a modification of the morphological sub-band decomposition algorithm proposed by Pei and Chen. In the first step, an input image is decomposed into four sub-bands using morphological opening and closing filters. In the second step, sub-bands are compressed with lossless methods matched to the dynamics of each sub-band. After transmission the sub-bands are decompressed and added together to form the output image. Results of computer simulations are presented.

1. Introduction

Expansion of computer networks during the last decade have caused drastic increase of information transferred by telecommunication links. A great part of this information are coded greyscale images. The problem of image coding and compression in order to decrease the amount of transmitted and stored information is therefore important. Many algorithms have been invented for coding and compression but most of them are complicated and require much processing time [1]. New fast and simple algorithms are still to be found. One of the possibilities is to use mathematical morphology as a tool for analysis of images and description of their structural properties [2]–[4]. As a result of morphological filtering performed in the image plane we calculate images which are simpler than the original and could be compressed with small compressed-to-original ratio.

A number of earlier experimental studies have shown the possibility of constructing optical-digital systems for morphological filtering [5]–[8]. The most time -consuming operation which is a convolution of an image with a filter running window can be made optically. Other algebraic and logical operations are then made in an electronic part of optoelectronic processors.

This paper presents advantages of using morphological operations to achieve fast image compression. The algorithm presented is a modified version of that proposed by PEI and CHEN [9]. The possibility of the algorithm being realized in an optical-digital systems is considered. In Section 2, we review mathematical morphology operations on binary and greyscale images. In Section 3, the sub-band decomposition operation in the image plane is defined, methods of compression of sub-bands are discussed, and a block diagram of the algorithm is presented. Section 4 contains the results of computer simulation.

2. Mathematical morphology

2.1. Basic morphological operations

Mathematical morphology is based on operations defined in set theory by Minkowski in the first decade of the 20-th century. These operations are Minkowski addition and subtraction. Symbols X and A denote any two sets in Euclidean space E.

Minkowski addition is defined as

$$X \oplus A = \{x+a : x \in X, a \in A\} = \bigcup_{a \in A} X_a = \bigcup_{x \in X} A_x \tag{1}$$

where $X_a = \{X+a : x \in X\}$ is the translation of a set X by a vector a.

Minkowski subtraction is defined as

$$X \ominus A = (X^c \oplus A)^c = \bigcap_{a \in A} X_{-a} = \bigcap_{x \in X} A_{-x} \tag{2}$$

where superscript c indicates the complement of a set, that is, $X^c = \{x \in E = \mathbf{R}^2 : \chi(x) = 0\}$, and χ is the characteristic function of a set X defined as follows:

$$\chi(x) = \begin{cases} 1 & \text{is } x \in X, \\ 0 & \text{otherwise.} \end{cases} \tag{3}$$

Let A^T be a set transposed to the set A, $A^T = \{-a : a \in A\}$. For a set symmetric with respect to its origin, the transposed set A^T is equal to itself. Then, basic morphological operations: erosion and dilation are defined as follows:

$$\varepsilon_{A^T}(X) = X \ominus A^T \quad - \text{ erosion,} \tag{4}$$

$$\delta_{A^T}(X) = X \oplus A^T \quad - \text{ dilation.} \tag{5}$$

One of the two sets, for example A, which is smaller, modifies structure of the set X, that is, it acts as a structuring element.

Another way of looking at erosion and dilation is that erosion ε_A of a set X by a structuring element A is a set of points (locus) in which the centre of the structuring element is located when the element A is included in the set X (in the extreme situation the set A is tangent to the boundary of the set X from inside); dilation δ_A of a set X by a structuring element A is a locus in which the centre of the structuring element is located when the element A intersects with the set X (in the extreme situation the set A is tangent to the boundary of the set X from outside).

This interpretation considered in terms of convolution of both binary functions gives erosion as supremum and dilation as infimum of the operation result.

Simple morphological filters, opening and closing ones, are calculated as sequences of erosion and dilation

$$X \circ A^T = (X \ominus A^T) \oplus A \quad - \text{ opening,} \tag{6}$$

$$X \bullet A^T = (X \oplus A^T) \ominus A \quad - \text{ closing.} \tag{7}$$

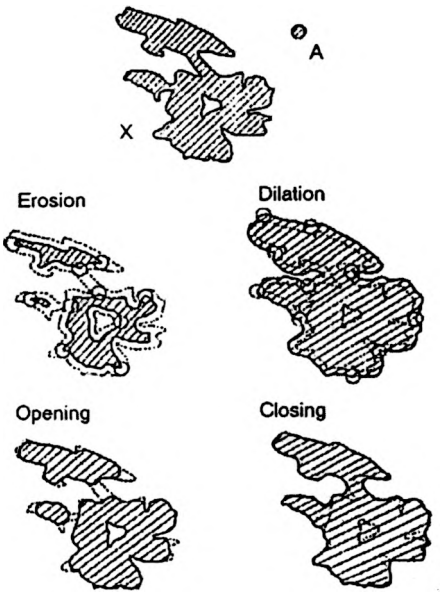

Fig. 1. Four basic morphological operations: erosion, dilation, opening and closing defined for binary sets.

The result of applying these morphological operations to sample binary set X is shown in Fig. 1.

2.2. Morphological operations on greyscale images

Basic morphological operations are defined for binary sets. Real-life images are greyscale, *i.e.*, are composed of various intensity values contained within a specified range. Thus, extension of morphological operations to the greyscale case is a natural need. According to the threshold decomposition concept this is done through slicing a greyscale image into binary intensity layers [10].

Image transformations are often divided into three groups [4]:

– SP (set processing), where a set represents a binary input and output image,

– FP (function processing), where a function represents a multi-level input and output image,

– FSP (function and set processing), which is a subgroup of FP, where the type on an output signal is the same as that of an input image (set–set or function–function).

Let us define the threshold decomposition for FSP transformations [10]. If φ is FSP transformation, Φ is corresponding SP transformation and χ_S is the characteristic function of a set S, then $\varphi(\chi_S) = \chi_{\varphi(S)}$. We say that φ fulfils threshold decomposition property if

$$[\varphi(f)](x) = \sup\{q \in V: x \in \Phi[T_q(f)]\} \tag{8}$$

where V is the set of f function values for any function f. Hence transformation of the function f by φ satisfying Eq. (8) is equivalent to its decomposition to the threshold

sets $T_q(f)$, transformation of each set $T_q(f)$ by Φ, and superposition of the output function from the transformed sets $\Phi[T_q(f)]$. FSP transformations are convenient for image analysis because they allow filtration of multi-level signals by means of binary signals transformation.

Threshold decomposition can be made on condition that FSP transformation φ commutes with thresholding for any function f

$$\Phi[T_q(f)] = T_q[\varphi(f)], \quad \forall q \in V. \tag{9}$$

Transformations which commute with thresholding are erosion, dilation, opening, closing and any combination of operations that commute with decomposition [10].

All morphological operations are non-linear signal transformations which locally modify their geometrical structure. Non-linearity of these operations results from thresholding local convolutions of structuring element and fragments of the input image at the maximum (erosion) or minimum (dilation) level.

3. Decomposition, compression and reconstruction of images using a morphological algorithm

3.1. Sub-band decomposition in the image plane

Two-dimensional (2D) Fourier transform (FT) plays an important role in the thoery of optical signals. Applied to a 2D input function, that is an image, FT generates another 2D function, which is representation of the image in terms of spatial frequencies. Small objects in the input image are related to high frequencies and large objects to low frequencies. This property is directional, *i.e.*, the object which is large along one direction and small along the perpendicular direction generates the spectrum with low and high orthogonal frequencies, respectively. The process of decomposition of 2D Fourier spectra to ranges which are connceted with objects that generate specified frequencies is called band filtration and these frequency ranges are called sub-bands.

Sub-band decomposition of images can also be performed in the image plane using morphological filters. In this case, the input image is called a band and its small size elements (objects) are called sub-bands. Morphological filters with structuring elements of controlled size and shape extract corresponding structures from the input image. In the 2D case morphological filtration of the image can be directional, that is, limited to one particular direction. Since 2D morphological and rank order filters are usually separable, a 2D filter can be decomposed to two 1D orthogonal filters.

In the image plane, decomposition of an image to sub-band allows faithful coding and decoding of images [11]–[14]. Each sub-band can be coded with small quantity of information for one pixel (measured in BPP – bits per pixel). This is because sub-bands contain objects that have similar structure. For example, high sub-bands contain large areas of constant values in highly correlated regions where there are no details in an input image.

As was shown in [11], the coding of images using sub-bands in the image plane has several advantages over other methods: 1) it gives high signal-to-noise ratio, 2) distortions of image are relatively small (considering resolution of the human eye), 3) it is simple and effective in applications.

3.2. Morphological analysis and synthesis filters

Morphological operations on an input image, which eliminate objects smaller than the size of a structuring element act like low-pass filters. Consequently, high-pass filters are calculated by subtraction of the result of low-pass filters from the original image. In this way, the analysis part of the sub-band decomposition system uses morphological filters with small structuring elements. Small structuring elements simplify digital calculation and allow easy optical implementation.

Morphological operations are advantageous for their effectivenss. In computers, these operations can be made very fast in comparison with other image processing operations. They can be be directly coded in VLSI circuits. Realisation of morphological operations in optical processors gives less exact results than those computer calculated. Small structuring elements correspond to small point spread functions, however, the speed of calculations does not depend on the size of structuring elements.

Most of the morphological algorithms require many operations, especially in digital systems. For example, dilation of an image composed of 512×512 pixels by a structuring element of 5×5 size needs 6,553,600 operations of comparsions. The algorithm proposed by PEI and CHEN [9] considerably simplifies decomposition to sub-bands in the case of 4 bands. This is achieved by reducing the number of algorithm steps. The idea of the algorithm is described below.

Let us denote by X the original image, γ and φ denote, respectively, opening and closing by 1D structuring element. Then, the 1D morphological low- and high-pass filters are constructed as follows:

$$\text{low-pass filter } H_0[X] = \varphi[\gamma[X]], \tag{10}$$

$$\text{high-pass filter } H_1[X] = X - H_0[X]. \tag{11}$$

In the low-pass filter, opening eliminates bright elements, which are smaller than the structuring element, then closing eliminates small dark elements. The high-pass filter is the difference between the original image and the result of low-pass filter. The output image contains only elements smaller than or equal to the size of a structuring element. In the 2D case we can take composition of the above filters calculated along vertical and horizontal directions, denoted by superscripts v and h, respectively:

$$\text{low-low } H_{00}[X] = H_0^v[H_0^h][X]], \tag{12}$$

$$\text{low-high } H_{01}[X] = H_0^v[H_1^h[X]], \tag{13}$$

$$\text{high-low } H_{10}[X] = H_1^v[H_0^h[X]], \tag{14}$$

$$\text{high-high } H_{11}[X] = H_1^v[H_1^h[X]]. \tag{15}$$

These filters decompose an image to 4 sub-bands of different structures which can be used for reconstruction according to the scheme shown in Fig. 2. Figure 3 presents an example of sub-band decomposition of a test binary image to show properties of the morphological algorithm. It should be noted that the resulting sub-bands are not binary because subtraction of intensities in Eqs. (12)–(15) may lead to both positive and negative values.

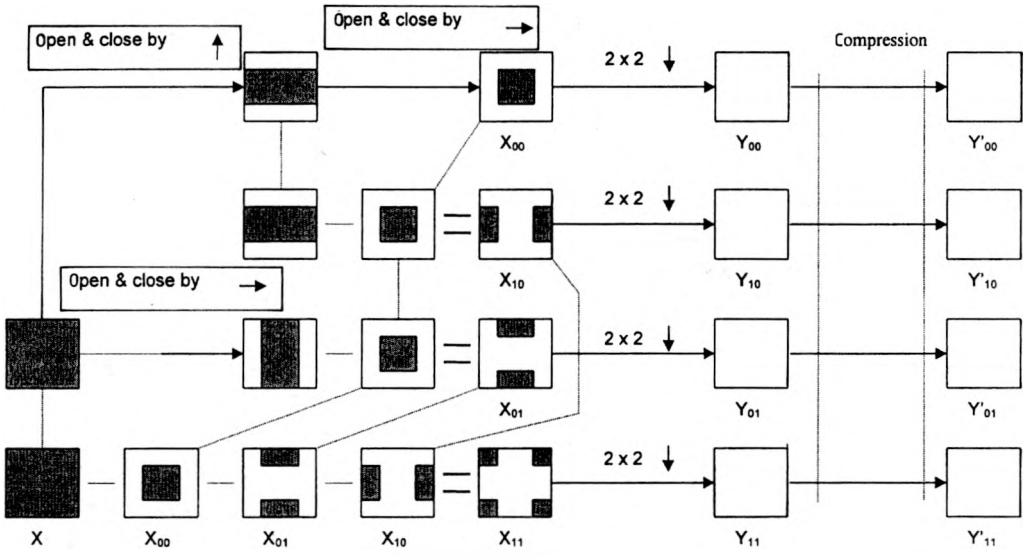

Fig. 2. Decomposition of the input image X to sub-bands X_{00}, X_{01}, X_{10}, X_{11}. After sampling sub-bands Y_{00}, Y_{01}, Y_{10}, Y_{11} are compressed to Y'_{00}, Y'_{01}, Y'_{10}, Y'_{11}.

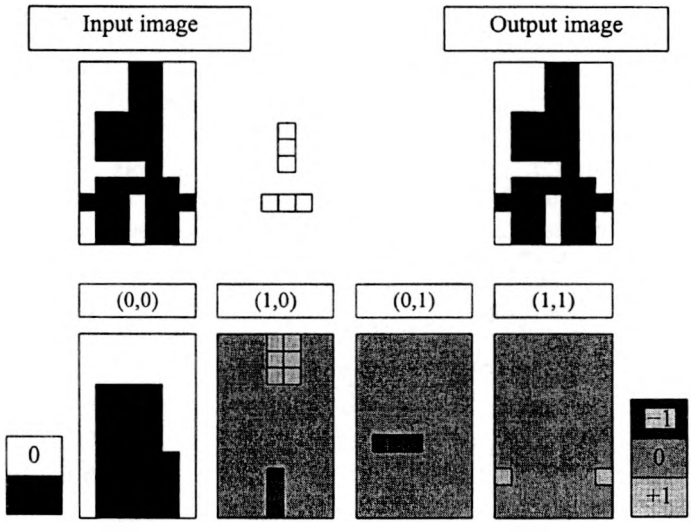

Fig. 3. Decomposition of a sample binary element to four sub-bands containing large as well as small horizontally or vertically oriented structures.

Due to subtraction, the sub-bands (1,0), (0,1) and (1,1), of either a binary or a greyscale image, may contain pixels of intensities, which are from outside of the input intensity range. To avoid an increase in the number of bits necessary to store the intensities their new values are scaled back to the previous range according to equation

$$x' = (x+n)\frac{Q}{(m+n)} \tag{16}$$

where m and n are the maximum positive and negative differences between intensities in the image ($m, n \geqslant 0$), respectively, Q denotes the number of grey levels used in the input image, x and x' are the values of intensity before and after scaling. Two structuring elements of sizes $1 \times p$ and $p \times 1$ are used, where $p = 3, 5, 7, 9, \ldots$.

Sub-band decomposition is performed using the scheme presented in Fig. 2. The system which produces sub-bands is composed of two parts: the analysis part in which several filters extract sub-bands from an input image (sub-bands contain only part of objects) and the coding part which prepares the sub-bands for transmission. In the coding part, pixel sampling is applied first to reduce information and then compresssion follows.

Decomposition requires 8 steps:

1. Elimination from the input image of objects which are smaller along the vertical direction than the structuring element $p \times 1$.

2. Elimination from the result of step 1 of objects which are small along the horizontal direction in comparison to the structuring element $1 \times p$. The result of the first two steps gives the sub-band (0,0).

3. Elimination from the result of step 1 of all objects except those which are larger in the vertical direction and smaller in the horizontal direction in comparison with those contained in the sub-band (0,0). The results of step 3 constitutes the sub-band (1,0).

4. Elimination from the input image of objects which are smaller in the horizontal direction than the structuring element $1 \times p$.

5. Elimination from the result of step 4 of all objects except those which are larger in the horizontal direction and smaller in the vertical direction in comparison with those contained in the sub-band (0,0). The result of step 5 gives the sub-band (0,1).

Steps 6–8 eliminate from the input image all the objects which belong to the sub-bands (0,1), (1,0) and (0,1), respectively. The results forms the sub-band (1,1).

Subsequently, four sub-bands are sampled in 2D with constant 2 to assure that the total number of pixels in all the sub-bands is not larger than the number of pixels in the input image. Hence, every sub-band is reduced to the area 4 times smaller than that of the input image.

Finally, the resulting sub-bands are compressed using the lossless Huffman coding.

In the reconstruction stage sub-bands are decompressed and then interpolated (Fig. 4) to the original size. Afterwards the sub-bands are added their intensities are

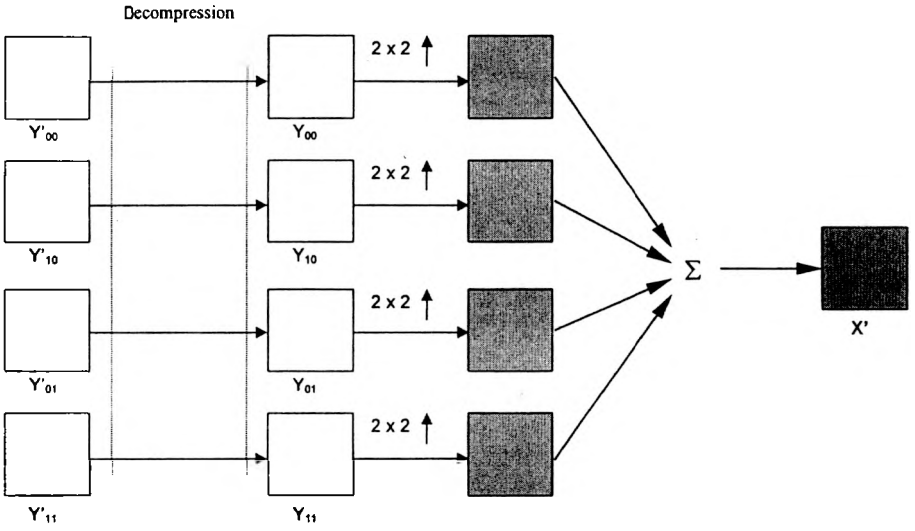

Fig. 4. Composition of the output image X' from sub-bands Y_{00}, Y_{01}, Y_{10}, Y_{11}.

normalised to obtain the output image with intensity values in the same range as those of the input image.

To achieve the best results of image analysis/synthesis the following two conditions should be satisfied:

1. The processing system should not introduce noticeable image distortion, that means, it should be resistant to quantization noise generated by sampling.

2. The system should not produce an output image of greater number of pixels than in an input image.

The algorithm presented in this paper is a simplification of that proposed by PEI and CHEN [9]. It does not require any morphological operations to reconstruct the output image from the sub-bands. In our algorithm, the reconstruction is a direct sum of interpolated sub-bands, scaled up to fit the original intensity range 0–255. This makes our algorithm fast and simple. Our experimental results seem to be better than those obtained when additional morphological operations are performed before the reconstruction of the output image [15]. The simplification proposed is important in the case when morphological sub-band decomposition of the input image is made in a fast photonic processor, sub-bands are transmitted through telecommunication links and then the output image is synthesised electronically. Recently, a demonstrator of the photonic system was reported, which could serve for morphological sub-band decomposition purposes [16], [17].

3.3. Image compression

The image plane sub-band decomposition produces a set of images with the total number of pixels bigger than in an original image. The total number of pixels in these sub-bands is reduced by sampling. Since the structure of sub-bands is very

regular, *i.e.*, highly correlated, it is possible to code the sub-bands with compression factor smaller than that possible in an original image.

The image plane sub-band (0,0) contains large elements which generate low spatial frequencies in the Fourier spectrum, because the pixels in this sub-band are highly correlated. This sub-band could be coded using one of the differential methods. Differential pulse code modulation (DPCM) method is frequently used. Moreover, due to the correlation of pixels the result is a sequence of small numbers which can be coded using smaller BPP ratio and then compressed using dictionary method, for example, Huffman coding [1].

The image plane sub-bands (1,0), (0,1), (1,1) contain small objects which generate high frequencies in the Fourier spectrum. Nevertheless, in these sub-bands there are still large areas of of pixels of similar intensities. Only some of the pixels mark edges and small objects. We can decrease the number of quantization levels and then apply a method which is effective for large areas of the same intensity, for exampe, run lenght encoding (RLE). The next step could be Huffman coding of the results.

Sampling the sub-bands (1,0), (0,1) and (1,1) causes relatively large loss of information in comparison with the sampling of the sub-band (0,0) which contains objects of sizes bigger than the sampling grid. All the objects from the latter sub-band are reconstructed in the output image although they can be shifted or distorted. This effect is not significant, however, on the contrary, removing pixels in the higher sub-bands causes blurring of edges and elimination of small objects. These effects should be analysed for each particular case of sampling the sub-bands.

4. Experimental results

In our computer simulation the input image of 512×512 pixels and 256 intensity levels was used. Due to subtraction performed in Eqs. (12)–(15), the sub-bands (1,0), (0,1) and (1,1) may contain pixels of intensities which are negative. In order that the number of bits necessary to store the new values of intensities be kept low, these are scaled back to previous 0–255 lavel range according to Eq. (16).

Since the sub-bands (1,0), (0,1) and (1,1) contain information mostly about edges, modification of intensities of pixels in these sub-bands is not significant for an observer. Therefore, we can modify histograms of these sub-bands decerasing the number of grey levels. Thus for all images the sub-bands of grey levels are limited to 16 according to the formula

$$q' = \begin{cases} 0 & \text{for } q = 0, \\ \dfrac{(15-1)}{(h-l)}(q-l)+1 & \text{for } q \subset (0;255] \end{cases} \tag{17}$$

where l and h are arbitrary threshold values. Almost all the pixels except those of value 0 are located between l and h. Histograms of the processed sub-bands show that this method gives the output image that is better than in the case of

quantization of intensity at equal intervals. However, it requires storing of the values l and h.

The sub-band (0,0) contains pixels which are highly correlated. Investigation of whether storing only the differences between pixels is beneficial or not resulted in a conclusion that the decrease of compression factor is not significant. The sub-bands (1,0), (0,1) and (1,1) contain pixels of similar intensities in large areas where the original image has neither edges nor small objects. However, almost invisible fluctuations of intensities make the RLE method useless. We find that the best compression factor is obtained for the Huffman coding method.

Figures 5a–f show, respectively: the input image, the output image and the sub-bands, all for the 1D structuring element of length 9. The structuring elements of lengths 3, 5, 7, 9, 15 and 21 pixels are also used. Two measures of the reconstruction error are used:

– mean absolute error (MAE) defined as

$$\mathrm{MAE} = \frac{1}{N}\sum_{\mathbf{k}} [I(\mathbf{k}) - \hat{I}(\mathbf{k}), \tag{18}$$

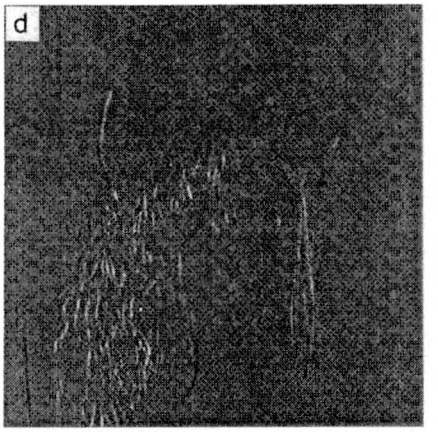

Fig. 5a–d

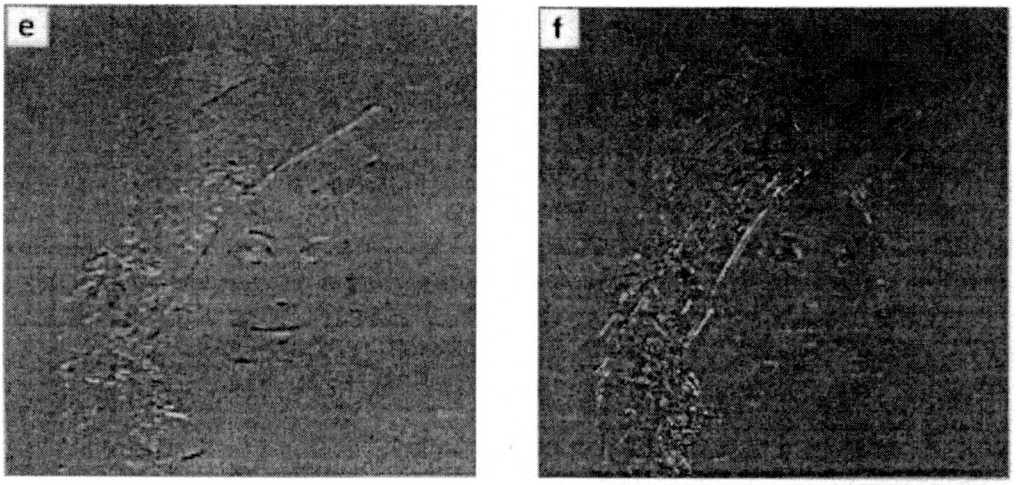

Fig. 5. Input image (a), output image (b), sub-band (0,0) (c), sub-bad (1,0) (d), sub-band (0,1) (e), sub-band (1,1) (f).

– maximum absoulte error (MAXAE) defined as

$$\mathrm{MAXAE} = \max\{I(\mathbf{k}) - \hat{I}(\mathbf{k})\}_{\mathbf{k}} \tag{19}$$

where I is the original image, $\hat{I}$ – the output image, $\mathbf{k}$ is the image point coordinate vector and N is the number of pixels in images.

Table 1. Compression factor, MAE and MAXAE for the test image with 256 grey levels.

Size of saturating element	Sub-bands compression factor	Output image compression factor	MAE	MAXAE
3 pixels	0.52 (4.16 bit/pxl)	0.32 (2.56 bit/pxl)	11.75	162
5 pixels	0.49 (3.92 bit/pxl)	0.33 (2.64 bit/pxl)	11.25	181
7 pixels	0.47 (3.76 bit/pxl)	0.32 (2.56 bit/pxl)	12.04	154
9 pixels	0.45 (3.60 bit/pxl)	0.32 (2.56 bit/pxl)	12.22	167
15 pixels	0.41 (3.28 bit/pxl)	0.33 (2.64 bit/pxl)	12.56	166
21 pixels	0.38 (3.04 bit/pxl)	0.32 (2.56 bit/pxl)	12.14	159

Table 2. Compression factor, MAE and MAXAE for the test image in the case of modification of histograms of sub-bands to 16 grey levels.

Size of saturating element	Sub-bands compression factor	Output image compression factor	MAE	MAXAE
3 pixels	0.38 (3.04 bit/pxl)	0.32 (2.56 bit/pxl)	10.17	161
5 pixels	0.33 (2.64 bit/pxl)	0.32 (2.56 bit/pxl)	10.87	149
7 pixels	0.31 (2.48 bit/pxl)	0.31 (2.48 bit/pxl)	11.00	158
9 pixels	0.28 (2.24 bit/pxl)	0.31 (2.48 bit/pxl)	10.46	159
15 pixels	0.24 (1.92 bit/pxl)	0.30 (2.40 bit/pxl)	11.52	170
21 pixels	0.21 (1.68 bit/pxl)	0.29 (2.32 bit/pxl)	12.30	155

Table 1 presents the quality of reconstruction in terms of the compression factor, MAE and MAXAE for the test image with 256 grey lavels. Table 2 shows the results obtained for sub-bands with reduced greyscale. For comparison purposes the tables show results of compression of the output image as well as the sub-bands.

5. Conclusions

Increasing the lenght of the structuring element causes the sub-band compression factors to decrease.The output image compression factor remains almost at the same level and is smaller than the compression factor of sub-bands on condition that the number of grey levels employed in the sub-bands is constant.

A decrease in the number of grey levels to 16 in the sub-bands (1,0), (0,1) (1,1) causes a significant decrease of sub-band compression factors while the output image compression factors remain almost the same.

MAE slightly increases with the structuring element size. In turn, a decrease in the number of grey levels causes a decrease of MAE. This result is quite unexpected because reduction of the dynamic range of intensities results in a loss of information. Besides, the images with reduced intensity range are worse from the visual point of view. This has led us to a conclusion that MAE should be cerefully used as a criterion for comparison of images processed in different ways.

For sub-bands with both 256 and 16 grey levels MAXAE preserves almost the same value with random changes independent of the size of structuring element.

Increasing the lenght of structuring element over 21 makes no sense. Its optimum length for 512×512 image size is $5-9$ pixels.

Further reduction of the compression factor should be achieved with efficient methods of sub-band coding. Differential and RLE methods are not the best ones in this case and need modification.

The main advantage of digital information processing is its flexibility. In the same experimental set-up any algorithm can be tested. The result can be copied, scaled, rotated and sent to other computers for use by other people interested in information about an image.

However, some operations in digital image processing are time-consuming. For example, the number of operations required to convolve two images is proportional to $n^2 \cdot m^2$, where n^2 is the number of pixels in the first image and m^2 in the second one. Thus, convolution of two images of 512×512 pixels size requires at least $7 \cdot 10^{10}$ arithmetic operations on pixel intensity values.

Such operations as convolution, vector–matrix and matrix–matrix products can be done in parallel in optical imaging systems. The disadvantage of optical systems lies in their lack of flexibility. Adjusting a shadow casting correlator takes some time.

To use only virtues of digital and optical processing it is advisable to combine both in photonic processors where optics is used to perform operations, which are time-consuming in digital realisation. A promising, fast and compact photonic system based on optical thyristors working in differential pairs has recently been

presented by BUCZYŃSKI *et al.* [16], [17]. The system was used as a hard clip thresholder of greyscale images and a morphological processor. At the moment, its drawbacks is a small size of processing matrices.

References

[1] SAYOOD K., *Introduction to Data Compression*, Morgan Kaufmann, Los Angeles 1996.
[2] MATHERON G., *Random Sets and Integral Theory*, Wiley, New York 1975.
[3] SERRA J., *Image Analysis and Mathematical Morphology*, Academic Press, London 1982.
[4] MARAGOS P., Opt. Eng. **26** (1987), 623.
[5] GARCIA J., SZOPLIK T., FERREIRA C., Opt. Lett. **18** (1993), 1952.
[6] SZOPLIK T., GARCIA J., FERREIRA C., Appl. Opt. **34** (1995), 267.
[7] GEDZIOROWSKI M., GARCIA J., Opt. Commun. **19** (1995), 207.
[8] SZOPLIK T. [Ed.] *Morphological Image Processing: Principles and Optoelectronics Implementations*, SPIE Milestone Series **127**, SPIE Optical Engineering Press, Bellingham 1996.
[9] PEI S.-C., CHEN F.-C., Opt. Eng. **30** (1991), 921.
[10] FITCH J.P., COYLE E.J., GALLAGHER N.C., IEEE Trans. Acoustics, Speech Signal Proc. **32** (1984), 1183.
[11] WOODS J.W., O'NEIL S.D., IEEE Trans. Acoustics, Speech Signal Proc. **34** (1986), 1278.
[12] GHARAVI H., TABATABAI A., IEEE Trans. Circuits and Systems **35** (1988), 207.
[13] TOET A., Pattern Recogn. Lett. **9** (1989), 255.
[14] PETERS II R.A., NICHOLS J.A., Proc. SPIE **2180** (1994), 163.
[15] PNIEWSKI J., SZOPLIK T., Proc. SPIE **3490** (1998), 115.
[16] BUCZYŃSKI R., BAUKNES V., SZOPLIK T., *et al.*, IEEE Photonics Techn. Lett. **11** (1999), 367.
[17] BUCZYŃSKI R., BAUKENS V., GOULET A., *et al.*, *Realization of mathematical morphology operations with an optoelectronic demonstrator system for early image processing*, 7th OSA Topical Meeting *Optics in Computing*, Proc., Snowmass Village–Aspen, Colorado, U.S.A., 1999.

Received May 22, 2000